

EFFECT OF MATERIAL PROPERTIES ON STRESS-INDUCED DEFECT GENERATION IN TRENCHED SOI

W.A. Nevin and K. Somasundram,
BCO Technologies (NI) Ltd., 5 Hannahstown Hill, Belfast BT17 0LT, N. Ireland, UK

S. Blackstone,
BCO America, P.O. Box 938, Durham, NH 03824-0938, USA

S. Magee and A.T. Paxton
Dept. of Pure and Applied Physics, Queen's University of Belfast,
Belfast, BT7 1NN, UK

ABSTRACT

We have investigated the influence of the material properties of the silicon device layer on the generation of defects, and in particular slip dislocations, in trenched and refilled fusion-bonded silicon-on-insulator (SOI) structures. A strong dependence on the ease of slip generation on the type of dopant species was observed, with the samples falling into three basic categories: heavily boron-doped silicon showed ready slip generation; arsenic and antimony-doped material was fairly resistant to slip; while silicon moderately or lightly doped with phosphorous or boron gave intermediate behaviour. The observed behaviour appears to be controlled by differences in the dislocation generation mechanism rather than by dislocation mobility. A relationship between dopant species and slip was also seen in SOI prepared with various implanted buried layers at the bonding interface. Here, the greatest slip occurred for both boron and antimony-implanted samples.

INTRODUCTION

Fusion bonded silicon-on-insulator (SOI) is becoming an increasingly important commercial substrate for the fabrication of electronic devices, such as bipolar and high-voltage structures (1,2). The buried oxide (BOX) incorporated at the bonding interface electrically isolates the top silicon layer from the thick substrate 'handle' layer, so that by trenching through the top layer to the BOX, and then lining the trench sidewalls with silicon oxide, electrically isolated tubs of silicon are formed, on which the devices can be fabricated. Advantages of these structures over conventional silicon substrates include reduced leakage currents and parasitic capacitances, reduced power consumption, faster switching speeds, high quality and versatility of the silicon layer type, and die shrinkage. While some SOI technologies, such as low-power CMOS (complimentary metal oxide semiconductor), are now relatively mature, the utilisation of SOI for high-voltage applications has been initially slower, but is rapidly gaining increasing attention, with

potential applications in a wide range of areas such as telecommunications and smart power (3,4).

A major problem for applying the trench-isolation technique to high-voltage structures is that the thickness of the sidewall oxide must be increased in order to give sufficient breakdown voltage. This leads to an increasing level of tensile stress exerted by the oxide on the silicon sidewall, which peaks close to the bottom corner of the trench, eventually leading to the generation of slip dislocations when the stress exceeds the yield strength of the material (4,5). This usually occurs during thermal cycling of the structures at high temperature, probably as a result of the difference in thermal expansion coefficient between the oxide and silicon. The degree of stress increases with increasing oxide thickness and decreasing tub size. An understanding of the effect of the silicon material properties on slip propagation is therefore important for both reducing the die size and increasing the obtainable trench isolation breakdown voltage.

In this work, we have investigated the influence of the material properties of the SOI device layer on the generation of slip dislocations in this layer at filled trenches, in particular by varying the type and concentration of dopant species in the material. We have also examined the effect of implanting buried layers of various dopant species on the degree of generation of slip dislocations from the bottom of the filled trenches.

EXPERIMENTAL

Starting device materials were polished 4" dia. silicon Czochralski (CZ) and float zone (FZ) wafers with various dopant species, dopant concentrations and crystal orientation, as summarised in Table I. For the implant-dependence study, SOI with buried implanted layers at the bonding interface were prepared by implanting 3-5 ohm.cm phosphorous-doped polished <100> CZ silicon device wafers with $5 \times 10^{15}/\text{cm}^2$, 80 keV doses of ions before joining. This gave a layer with a dopant concentration of about 5×10^{19} atoms/cm³ in the device close to the bonding interface, after the final stage of sample processing. The handle material was 3-5 ohm.cm phosphorous-doped polished CZ silicon with <100> crystal orientation. A 1.0 μm thick thermal oxide layer was grown on the handle wafers before bonding, which formed the buried oxide of the SOI wafer. The bonded SOI samples were prepared by joining the device and handle wafers at room temperature following a modified RCA clean, and bond annealing at 1050°C. The device layer was then thinned to 20 μm by grinding and chemical-mechanical polishing, patterned using standard photolithographic techniques, and 3 μm wide trenches etched to the buried oxide using an inductively coupled plasma etching method (6). The angle between the trench sidewall and the surface plane was close to 90°.

Slip dislocation generation was examined by refilling the trenches and thermally stressing the samples by annealing at high temperature. The full refill process consisted of first lining the trenches with a thick layer of low-pressure chemical vapour deposited (LPCVD) TEOS (tetraethoxy silane) oxide deposited at 700°C, then filling the centres with LPCVD polysilicon at 650°C, planarising the polysilicon, capping the trench top with a further LPCVD oxide layer, and annealing at 1050°C for 1 h in nitrogen at two stages of the refill process (see Scheme 1). The thermal annealing resulted in densification and shrinkage of the oxide films by around 5%. The degree of generated slip during the refill was analysed by inspecting the SOI surface using phase-sensitive Nomarski optical microscopy, and at the end of the process by Secco etching of cross

sections. Four to eight samples were processed in each group of wafers. The degree of slip was estimated for each wafer as a percentage of die affected by slip, measured along two lines across the entire wafer diameter, perpendicular and parallel to the flat, bisecting at the wafer centre (one affected tub in a die constituted a positive count). The total number of die along these lines was 81, and the dimension of each die was about 1 mm square. To allow for an observed wafer-to-wafer variation, the slip was taken as the average value of all the wafers in a given group.

In order to study oxygen precipitation behaviour in the device wafers, untrenched SOI were thermally oxidised in wet oxygen at 1050°C, to grow a 500 nm thick oxide layer. Secco etching was then used to delineate the oxidation-induced defects and these were examined by Nomarski microscopy.

RESULTS AND DISCUSSION

Results of slip inspections at the processing stages of post oxide liner deposition, post liner densification and post final oxide densification are listed in Table I. We observed a strong dependence of the ease of slip generation on the type of dopant species in the silicon device material. In the heavily boron-doped samples, a high level of slip was found immediately after deposition of the CVD oxide liner, as seen in the Nomarski micrograph of Figure 1a. Similarly to previous studies (5), the slip emanates from high-stress regions near the bottom corners of the trenches, propagates along the Si $\langle 111 \rangle$ plane, and is seen at the surface as lines running parallel to the trenches. This was verified by Secco etching cross-sections of the wafers, which showed an angle of 50-54° between the slip line and the wafer surface, which is similar to the angle between the $\langle 100 \rangle$ and $\langle 111 \rangle$ crystallographic planes. In contrast, the other material groups showed little or no slip at the liner deposition stage, but the degree of slip was then seen to increase with each high-temperature annealing cycle. For example, the degree of slip in the slightly-doped (1×10^{14} atoms/cm³) phosphorous samples increased from 7% at liner deposition, to 42% at liner densification, to 53% after the final densification. The arsenic and antimony wafers had more resistance to slip, with one of the antimony groups remaining entirely slip-free through the complete trench refill and thermal cycling (see Fig. 1b). Secco-etching of cross-sections confirmed the absence of slip in this case.

No obvious trends in ease of slip generation were seen between the FZ and CZ growth types and between the $\langle 100 \rangle$ and $\langle 111 \rangle$ orientations. The $\langle 111 \rangle$ wafers, did however show additional slip lines running diagonally across the tubs, as shown in Fig. 1c. This would be a concern for fabricating devices, since it would be more difficult to design device components outside the slip areas in this case compared to samples with $\langle 100 \rangle$ orientation.

We refer our discussion to Figure 2, which shows the percentage slip after final densification plotted against the dopant concentration. There is clearly no correlation between these. Indeed the general trends are opposite to those one might anticipate from the known dependence of yield stress or dislocation velocity on doping, or more precisely on the position of the Fermi level (7). Briefly, Hirsch's theory (8) supposes that the activation energy for the formation of kink pairs is lowered if the kinks are charged. Given that there are deep levels associated with these kinks, the concentration of charged kinks will depend on the position of the Fermi level. Thus, in general, yield strength will be greater or less as the concentration of dopant atoms increases in p- and n-type Si,

respectively. Therefore, if the Fermi level were determined by the doping level one would expect a positive slope in the data in Figure 2, except for the B-doped samples for which the slope would be negative.

However, slip in these experiments is almost certainly occurring at temperatures between 700 and 1050°C, and at these temperatures the Fermi energy is pinned at approximately mid-gap by the large intrinsic carrier concentration. This is true for all samples with concentrations less than $10^{18}/\text{cm}^3$. Hence, we do not believe the effect of the doping level upon slip generation to be an electronic effect in the sense of the Hirsch theory. We expect the dislocation mobility to be approximately the same in all samples at the temperature of deposition and densification. We suppose, therefore, that slip generation is controlled by dislocation generation rather than mobility.

With this in mind, we regard the data in Figure 2 to fall into three categories:

1. The $9 \times 10^{18}/\text{cm}^3$ B-doped specimens slip readily after only liner deposition. These were also the only specimens to show a high density of oxygen-related defects after thermal oxidation ($9 \times 10^5/\text{cm}^2$, compared to around $2 \times 10^3/\text{cm}^2$ for the other groups). The generation of these defects is known to be enhanced in heavily B-doped Si, and to nucleate dislocations during precipitation by prismatic punching (9). Therefore, in these samples a high dislocation density was created during the bond-anneal processing, leading to a resulting high incidence of slip.

2. The remaining B- and all the P-doped samples fall into a second category, showing some 40-80% slip with no clear dependence on dopant concentration. Two B-doped specimens with similar dopant concentration nevertheless showed a large disparity in amount of slip. The P-doped specimens with a concentration of $1.4 \times 10^{14}/\text{cm}^3$ are essentially intrinsic, and we expect all the crystals to be practically dislocation free as received. We propose that the slip generation is controlled by dislocation generation at the Si-SiO₂ interface. Therefore, the amount of slip generation in this category reflects the ability of the Si-SiO₂ interface in intrinsic materials to nucleate dislocations under stress.

3. The As- and Sb-doped samples fall into the third category whose slip generation is much less, even than the intrinsic Si. Assuming our postulate that slip is generated by dislocation nucleation at the Si-SiO₂ interface, we expect that As and Sb are able to inhibit dislocation nucleation by some mechanism currently not understood.

The picture we have, therefore, is that large stresses due to mismatch in thermal expansivity arise at the Si-SiO₂ interface which are relieved by slip. Measurements by Baumgart et al. (4) have shown tensile stresses as large as 500 MPa in trench isolation structures similar, although smaller, than ours. Except for the heavily B-doped samples the dislocation density is too low to allow general yielding, and the amount of slip is controlled by the ease of dislocation nucleation at the Si-SiO₂ interface. It is possible that As and Sb segregate to the interface and inhibit dislocation nucleation.

Table II summarises the slip results for the SOI with buried implants. Two features are apparent: the unimplanted samples remain slip-free throughout the process, while the implanted groups show varying degrees of slip, depending on the species type. However, in this case, the dependence on dopant type is different than that seen in Table I, with both the Sb- and B-implanted wafers being worse than P- and As-implanted samples. Clearly, the introduction of a heavily-doped implanted layer must weaken the

silicon material close to the bonded interface. This may be due to residual crystalline damage caused during the implant which has been insufficiently annealed, or to stress in the silicon from the presence of the dopant atoms. In this respect, there is more deviation from the Si-Si bond length for both Si-Sb (larger) and Si-B (smaller bond length) compared to Si-P and Si-As, which are fairly close to Si-Si. The effect does not appear to be related to oxygen precipitates, since all the implanted samples showed similar, low levels of the order of 10^3 defects/cm² after thermal oxidation.

Further work must concentrate on the Si-SiO₂ interface in order to characterise its atomic structure and chemical composition in doped structures. It is known that the interface is rather abrupt, that the Si is stepped, and that there is possibly a layer of SiO stoichiometry (10). It is likely that dislocations nucleate as loops at the steps and expand into the Si crystal. We cannot say at this stage how this process depends on interface characteristics or composition.

CONCLUSIONS

We have observed a strong dependence of the ease of generation of slip dislocations on the type of dopant species in the silicon device material in trenched and refilled fusion-bonded SOI wafers. The material studied fell into three categories: (1) Slip generation occurred very easily in heavily B-doped material, being seen at the oxide liner deposition stage. This appears related to a high density of oxygen precipitate-related defects grown during the high-temperature bond anneal. (2) Samples with moderate to low concentrations of B or P showed increasing degrees of slip as the wafers were processed through the refill and thermal annealing cycles. However, there appeared to be little dependence on the dopant concentration. (3) As- and Sb-doped materials were much more resistant to slip than the other materials, with Sb samples showing no slip through the complete process. The slip behaviour of groups (2) and (3) could not be explained by conventional dislocation mobility theory, but rather the lower occurrence of slip in group (3) appears due to an inhibition of dislocation nucleation in the stressed regions. No apparent influence of growth type (CZ vs. FZ) or crystal orientation (<111> vs. <100>) on the ease of slip generation was seen. Implanting a layer of dopant into the device at the bonding interface resulted in a significant softening of the material, with B and Sb implants giving higher slip generation than P and As species.

Further work on determining the reasons for the observed differences in behaviour should focus on examining the structural and chemical characteristics of the Si-SiO₂ trench-sidewall and bonding interfaces.

ACKNOWLEDGMENTS

We are grateful to Mike Finnis of the Queen's University of Belfast for useful discussions.

REFERENCES

- (1) Q.-Y. Tong and U. Gösele, *Semiconductor Wafer Bonding: Science and Technology*, Wiley Interscience, New York (1999).
- (2) F. Udrea, D. Garner, K. Sheng, A. Popescu, H.T. Lim, and W.I. Milne, *Electronics and Communication Eng. J.*, p. 27 (Feb., 2000).
- (3) N. Polce, M. Calley, S. Jones, S. Blackstone, and P. Martin, in *Semiconductor Wafer Bonding: Science, Technology and Applications V/1999*, C.E. Hunt, H. Baumgart, T. Abe, and U. Gösele, Editors, PV 99-35, The Electrochemical Society Proceedings Series, Pennington, NJ (2000).
- (4) H. Baumgart, T.J. Letavic, I. De Wolf, L. Tsou, H.E. Maes and R. Egloff, in *Semiconductor Wafer Bonding: Science, Technology and Applications III/1997*, U. Gösele, H. Baumgart, T. Abe, C. Hunt, and S. Iyer, Editors, PV 97-36, p. 440, The Electrochemical Society Proceedings Series, Pennington, NJ (1998).
- (5) C.S. Cowen, D.R. Craven, C.A. Goodwin, C.-M. Hsieh, G.T. Jones, and T. Pandhumsoporn, in *Silicon-on-Insulator Technology and Devices VII/1996*, P.L.F. Hemment, S. Cristoloveanu, K. Izumi, T. Houston, and S. Wilson, Editors, PV 96-3, p. 364, The Electrochemical Society Proceedings Series, Pennington, NJ (1996).
- (6) C. Gormley, K. Yallup, W.A. Nevin, J. Bhardwaj, H. Ashraf, P. Huggett, and S. Blackstone, in *Semiconductor Wafer Bonding: Science, Technology and Applications V/1999*, C.E. Hunt, H. Baumgart, T. Abe, and U. Gösele, Editors, PV 99-35, The Electrochemical Society Proceedings Series, Pennington, NJ (2000).
- (7) P.B. Hirsch, P. Pirouz, S.G. Roberts, and P.D. Warren, *Inst. Phys. Conf. Ser. No. 27*, Chap. 2, p.83 (1986).
- (8) P.B. Hirsch, *J. Physique*, 40, Coll C6, 117 (1979).
- (9) T. Ono, A. Romanowski, E. Asayama, H. Horie, K. Sueoka, H. Tsuya, and G.A. Rozgonyi, *J. Electrochem. Soc.*, 146, 3461 (1999).
- (10) N.F. Mott, *Phil. Mag. B*, 55, 117 (1987).

SCHEME 1. Trench refill, annealing and slip inspection sequence.

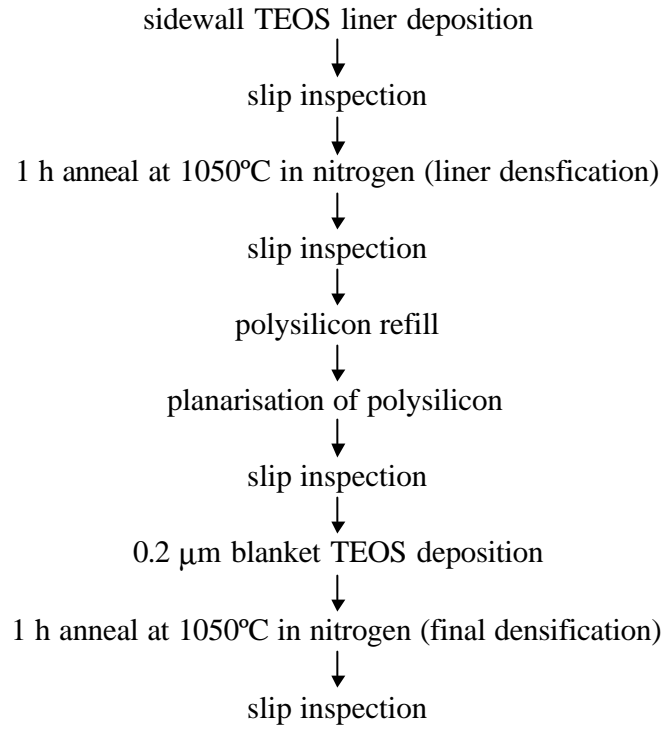


TABLE I. Properties of device material used for SOI fabrication, and results of slip inspections in trenched samples with a 1.1 μm thick oxide liner.

Material properties					Degree of Slip (%)		
Dopant	Concentration (atoms/cm ³)	Resistivity (ohm.cm)	Growth Type	Orientation	Liner dep.	Liner dense	Final dense
B	9.0×10^{18}	0.01	CZ	<100>	96	100	100
B	9.5×10^{14}	14	CZ	<100>	0	13	39
B	3.8×10^{14}	35	CZ	<100>	0	38	69
P	8.0×10^{16}	0.1	FZ	<111>	4	69	75
P	1.1×10^{15}	4	FZ	<100>	0	60	78
P	1.4×10^{12}	3000	FZ	<111>	7	42	53
As	8.0×10^{18}	0.007	CZ	<100>	0	9	20
As	4.5×10^{18}	0.01	CZ	<111>	0	4	12
Sb	2.4×10^{17}	0.05	CZ	<100>	0	0	0
Sb	2.8×10^{17}	0.04	CZ	<111>	0	5	10

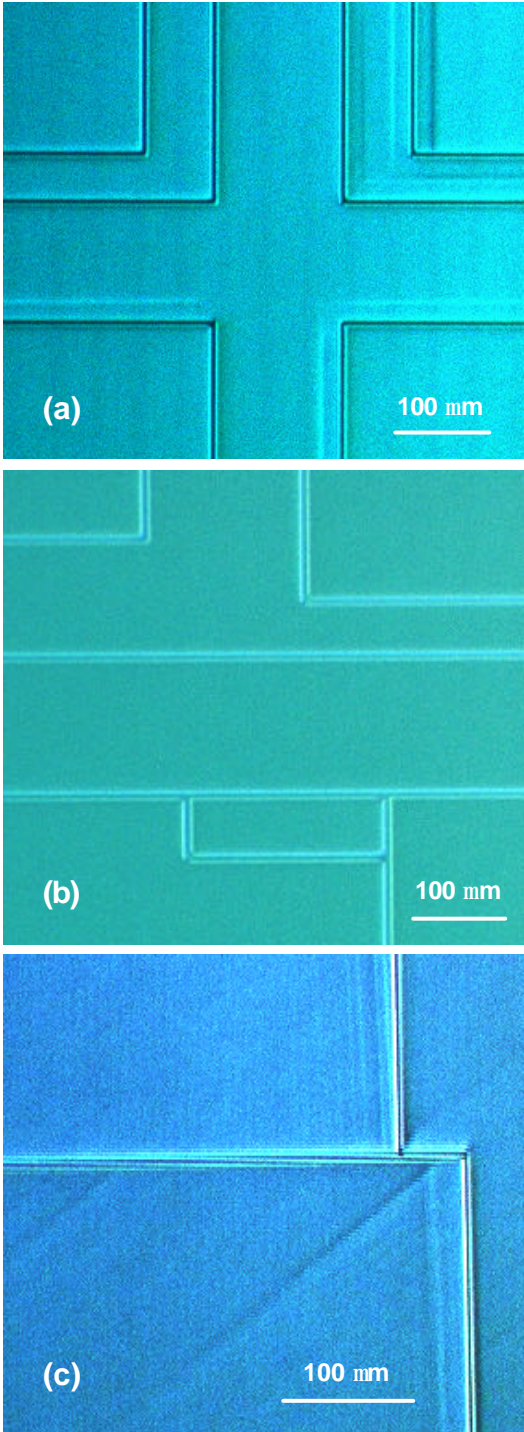


Fig. 1. Nomarski images of the surfaces of trench SOI samples with (a) B-doped $\langle 100 \rangle$, (b) Sb-doped $\langle 100 \rangle$ and (c) P-doped $\langle 111 \rangle$ silicon.

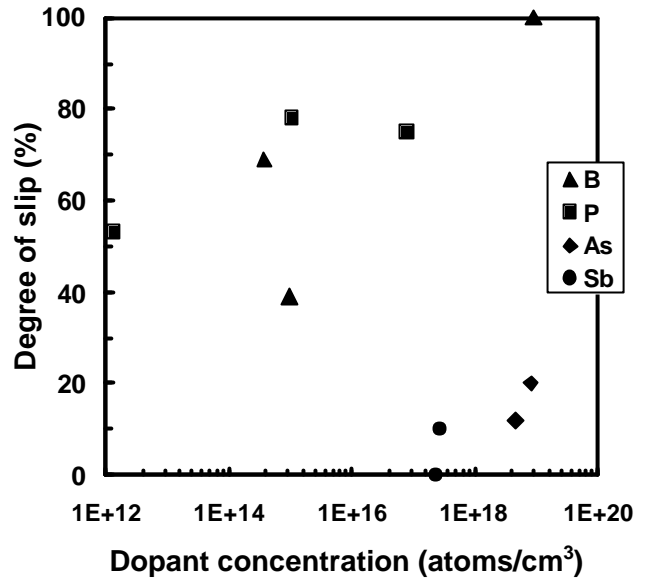


Fig. 2. Degree of slip after final densification as a function of doping concentration for trench SOI samples with various device layer dopants.

TABLE II. Dependence of slip generation on buried implant species in trench SOI with a $0.55 \mu\text{m}$ thick oxide liner.

Implant Species	Degree of Slip (%)		
	Liner dep.	Liner dense	Final dense
none	0	0	0
B	0	100	100
P	0	43	47
As	0	48	49
Sb	0	88	100